scientific reports

Check for updates

OPEN

The impact of ERAP1 inhibition on metabolite homeostasis of melanoma cells

Aroosha Raja[1,6], Martha Nikopaschou[2,3,6], Joke H. de Boer[1], Jeannette Ossewaarde-van Norel[1], Anna Artati[4], Michael Witting[4,5], Efstratios Stratikos[2,3,7]✉ & Jonas J. W. Kuiper[1,7]✉

Manipulation of the activity of Endoplasmic Reticulum AminoPeptidase 1 (ERAP1) has emerged as a powerful tool for the modulation of the cellular antigenicity and concomitant adaptive immune responses, with potential applications in cancer immunotherapy and Major Histocompatibility class (MHC)-associated autoimmunity being explored. Small molecule inhibitors often target allosteric sites of ERAP1 to achieve superior selectivity. However, recent findings suggested that ERAP1 functional perturbation may also affect cellular metabolism, raising concerns on the safety of this approach. To address this, we treated a melanoma cancer cell line with near saturating doses of an allosteric ERAP1 inhibitor and compared metabolite homeostasis to untreated and knock-out cells. Analysis of 8625 detected metabolite features revealed non-significant changes in metabolite composition in both inhibitor concentrations tested and only small changes in the ERAP1 knockout (KO) cells, limited to up to 25 metabolite features, most notably choline. Our results suggest that pharmacological inhibition of ERAP1 that targets allosteric sites, does not induce sufficiently large metabolic shifts to alter metabolite homeostasis. This is distinct from genetic deletion of the protein, which induces additional effects, albeit limited. These results encourage the exploration of allosteric ERAP1 inhibitors as pharmacological agents for the modulation of immune responses in the clinic.

Endoplasmic Reticulum Aminopeptidase 1 (ERAP1) is a metallo-aminopeptidase that trims N-terminally extended precursor peptides in the endoplasmic reticulum (ER). ERAP1-mediated trimming can optimize peptide binding to Major Histocompatiblity class (MHC) I molecules for CD8 + T cell recognition, but excessive trimming may generate peptides that no longer bind MHC class I, resulting in the loss of potential epitopes. Several genome wide association studies have correlated *ERAP1*gene variants with chronic inflammatory conditions collectively known as MHC-I-opathies, often in epistasis with specific MHC-I haplotypes[1]. In addition, ERAP1 activity has been shown to influence anti-tumor immune responses by regulating the repertoire of peptides presented to T lymphocytes and Natural Killer (NK) cells[2–4]. For these reasons, modulating its activity has emerged as a promising therapeutic strategy to restore normal immune surveillance or enhance anti-tumor immune responses[5–7]. Pharmacological inhibition of ERAP1 activity may prevent the destruction of putative immunogenic peptides, enhancing $CD8^+$ T-cell recognition of tumor-derived epitopes. Conversely, mutations that affect ERAP1 expression or enzymatic activity in tumor tissue can alter the balance between epitope generation and destruction, reducing effective MHC class I presentation and facilitate tumor immune evasion through impaired $CD8^+$ T-cell recognition and elimination, thereby facilitating tumor growth and expansion[5,6].

Initial efforts to target ERAP1 pharmacologically with small molecule inhibitors have mainly focused on the enzyme's active site[8]. However, the high degree of homology between ERAP1 and other closely related aminopeptidases has posed significant challenges in achieving selective inhibition[9,10]. To solve this problem, efforts have shifted to allosteric sites, including the malate and bis-tris-propane binding pockets, which offer distinct structural features that can lead to selectivity[11]. Indeed, library screening approaches led to the

[1]Department of Ophthalmology, Center for Translational Immunology, University Medical Center Utrecht, Utrecht University, Heidelberglaan 100, 3584 CX Utrecht, The Netherlands. [2]Department of Chemistry, National and Kapodistrian University of Athens, Panepistimiopolis Zographou, 15772 Athens, Greece. [3]National Centre for Scientific Research Demokritos, Agia Paraskevi, 15341 Athens, Greece. [4]Metabolomics and Proteomics Core, Helmholtz Zentrum München, Neuherberg Munich, Germany. [5]Chair of Analytical Food Chemistry, TUM School of Life Sciences, Technical University of Munich, Freising-Weihenstephan, Germany. [6]Aroosha Raja and Martha Nikopaschou contributed equally to this work. [7]Efstratios Stratikos and Jonas J. W. Kuiper contributed equally to this work. ✉email: estratikos@chem.uoa.gr; j.j.w.kuiper@umcutrecht.nl

identification of compound 3 [(4-methoxy-3-(N-(2-(piperidin-1-yl)-5-(trifluoromethyl)phenyl)sulfamoyl) benzoic acid], which was demonstrated by docking and mutagenesis studies to bind specifically to the bis-tris-propane allosteric site of ERAP1. Compound 3 exhibited strong selectivity for ERAP1 over related enzymes and showed reasonable potency in cellular models, with an effective dose (ED_{50}) of 1 μM[12]. Consequently, it has become a valuable tool molecule in investigating ERAP1 pharmacology and the biological consequences of its inhibition across multiple studies[13–16]. In our recent exploration using compound 3 to disrupt ERAP1 function in A375 melanoma cells, as well as an ERAP1 knock out (KO) clone of the same cell line, proteomic profiling uncovered alterations in the cellular proteome alongside limited metabolic adaptations related to endoplasmic reticulum (ER) stress and mitochondrial function. These alterations were more profound in ERAP1 KO cells. Although no overall toxicity was observed, these findings raised important considerations regarding potential off-target effects, particularly in cancer cell metabolism[13].

Given these observations, we investigate here whether ERAP1 inhibition and silencing induce more subtle metabolic dysfunctions by employing non-targeted metabolomics, an increasingly adopted approach to detect sublethal metabolic perturbations caused by therapeutic agents[17,18]. This method enables a more sensitive evaluation of metabolic adaptations or stress responses that may not manifest as immediate toxicity but could impact long-term cell viability and function. In our analysis, we find only limited effects from the ERAP1 KO and no significant changes induced by the allosteric inhibitor, suggesting that any metabolic adaptations to ERAP1 inhibition are not reflected to metabolite homeostasis and highlighting the potential safety of targeting this allosteric site for pharmacological applications aiming to regulate adaptive immune responses.

Methodology

Cell culture

A375 wild type (CRL-1619, ATCC) and ERAP1 KO cells (Clone 1B12, previously generated in house[19] were cultured in Dulbecco's Modified Eagle Medium containing high glucose, L-glutamine and sodium pyruvate (DMEM, Biowest, L0104), 10% fetal bovine serum (FBS, Biowest, S1810) and 1% Penicillin-Streptomycin (Biowest, L022) at 37 °C with 5% CO_2.

Inhibitor treatment and sample preparation for non-targeted metabolomics experiment

ERAP1-component and ERAP1-deficient A375 cells were seeded in a 6-well plate at a cell density of 140,000 c/ml (280,000 c/well) and cultured for 24 h. We then treated cells for 48 h with ERAP1 inhibitor (4-methoxy-3-(N-(2-(piperidin-1-yl)- 5-(trifluoromethyl)phenyl)sulfamoyl)benzoic acid) at concentrations of 0, 10, or 50 μM, dissolved in 0.1% DMSO. Subsequently, cells were washed twice with PBS and 400 μl of ice-cold extraction solvent (80% methanol in LC-MS/MS grade water cooled with dry ice) was added per well. Cells were detached with a rubber-tipped scraper and the cell suspension was transferred into a precooled cryovial held on dry ice. The well was then washed with 200 μl extraction solvent and pooled into the same cryovial to recover any remaining cells. Samples were immediately stored at -80 °C until measurement.

LC-MS/MS based non-targeted metabolomics

Analysis has been performed using Hydrophilic Liquid Interaction Chromatography as described recently[20]. Briefly, two different methods have been used on an Agilent 1290 Infinity II BioLC (Agilent Technologies, Waldbronn, Germany) coupled to a Sciex ZenoTOF 7600 (Sciex, Darmstadt, Germany). In case of positive ionization mode, metabolites are separated on an Agilent Infinity Poroshell 120 HILIC (100 mm × 2.1 mm ID, 2.7 μm particle size, peek-lined) using a linear gradient from eluent B (10% H_2O/90% ACN + 10 mM ammonium formate/0.1% formic acid) to eluent A (100% H_2O + 10 mM ammonium formate/0.1% formic acid). For negative ionization mode, metabolites were separated using a Waters Atlantis Premier BEH Z-HILIC (100 mm × 2.1 mm ID, 1.7 μm particle size) using a linear gradient from eluent B (10% H_2O/90% ACN + 10 mM ammonium acetate, pH 9) to eluent A (100% H_2O + 10 mM ammonium acetate, pH 9). The MS system was automatically recalibrated every 5 injections. Processing of the obtained data was performed in mzmine 4.7.27 and exported for further processing in R. After, non-targeted metabolomic analysis of 6 biological replicates per condition, the metabolite feature areas were normalized by cell amount using the Hoechst Assay. Metabolite features were filtered using pooled quality control from the cells (CMTRX) or a long-term reference plasma (MTRX). To be retained, a feature had to meet the following criteria: it was detected in all replicates, had a relative standard deviation (RSD) ≤ 30%, and showed a signal at least 1.5 times higher than the blank in at least one group (CMTRX or MTRX). Additionally, only metabolites with valid intensity measurements in at least 70% of samples were kept for further analysis. Metabolites were annotated by comparison against an in-house reference database, as well as external MS2 databases.

Data preprocessing and statistical analyses

We analysed 28 samples across five conditions, including reference controls (CMTRX, $n = 4$), ERAP1-competent cells without inhibitor (control, $n = 6$), cells treated with 10μM ERAP1 inhibitor (moderate, $n = 6$), cells treated with 50μM ERAP1 inhibitor (high doses, $n = 6$), and ERAP1 knockout cells (KO, $n = 6$). Reference samples were used for quality control (QC) but excluded from comparisons between the groups, resulting in $n = 6$ per group for all statistical comparisons (24 experimental samples total). In positive ionization mode, 49.4% of metabolite features had missing values and 24.3% in negative mode. All variables were continuous.

After QC, missing values were imputed using *Multiple Imputation by Chained Equations* (MICE) with random-forest predictors[21]. This iterative, multivariate approach fits a non-parametric random-forest model for each variable with missing data, using the observed values of other variables to predict and replace missing values while preserving inter-variable relationships. We generated three imputed datasets (m = 3) using a random forest with 100 trees with maximum 10 iterations to achieve convergence, and a fixed random seed (500) for reproducibility. To assess robustness, we performed sensitivity analyses comparing random forest imputation with predictive mean matching. Results showed high concordance between methods (mean correlation > 0.94 in positive mode, > 0.97 in negative mode), supporting the robustness of our imputation strategy. Next, we scaled the data using *Variable Stability Scaling* (VAST)[22] to stabilise the variance across variables while preserving the metabolites having higher mean intensities. VAST scaling reduces noise from low-abundance features and improves comparability across variables. Principal Component and Partial Least Squares Discriminant analyses (PLS-DA) were performed on the imputed dataset for exploratory visualisations using the *prcomp* function from *FactoMineR*[23] package and *plsda* function from *mixOmics R*[24] package, respectively. We also calculated variable of importance (VIP) scores from PLS-DA projections to determine the most discriminating metabolites differentiating between conditions. Subsequently, we applied an empirical Bayes–informed linear model using the limma package[25]. This approach is particularly suitable for small sample sizes ($n = 6$ per group), as it stabilizes variance estimates and increases statistical power while controlling the false discovery rate. The analysis was performed independently on each of the three imputed datasets, after which the results were combined using Rubin's rules, ensuring that imputed values were not treated as true observations. For each metabolite feature, an independent linear model was fitted with treatment group as the categorical predictor ($n = 6$ per group), resulting in one model per metabolite (4948 in positive and 3677 in negative ionization mode). A no-intercept design (Expression ~ 0 + Group) was used to directly estimate group means and enable all pairwise comparisons between treatment conditions. This method identified metabolites (by statistical inference) that are significantly different between the experimental conditions. We applied empirical Bayes shrinkage to increase the statistical power and *P*-values were subsequently adjusted using the Benjamini Hochberg method[26], to control the false discovery rate (FDR). We visualized the distributions and group differences of key annotated metabolite features using boxplots and performed one-way ANOVA for exploratory comparison of metabolite concentrations between the study groups. Given the limited sample size ($n = 6$ per group), *P* values derived from the ANOVA analyses should be interpreted as exploratory. We used the *RefMet*[27] and the *Human Metabolome Database*[28] for pathway analyses, superclasses, classes and chemical structures of the annotated metabolite features. We applied the same methodology to both the positive and negative modes of the metabolomics data.

Results and discussion

ERAP1 was knocked out in A375 cells using CRISPR–Cas9 as described previously[13,19]. We performed SNP-array analysis to screen for off-target copy-number changes introduced during knockout. No genome-wide duplications or deletions attributable to the knockout were detected.

To characterize the metabolomic profile of *ERAP1* knockout cells (KO) and compare this to ERAP1-component cells without treatment (control) or with 10 mM (moderate) or 50 mM (high) doses of ERAP1 inhibitor (6 replicates each), we performed LC-MS/MS based non-targeted metabolomics (Fig. 1A). In total, 4948 and 3677 metabolite features were detected with non-zero peak areas across all the replicates from the positive and negative ionization modes, respectively. A Principal component Analysis (PCA) of all detected features (> 4,000) revealed that the metabolic profiles of each condition were highly comparable, indicating that metabolic pathways are not significantly altered in the inhibitor treated cells (Fig. 1B). To detect potential minor metabolomic changes between the conditions, we used Partial Least Squares Discriminant Analyses (PLS-DA) with variable importance Analysis (VOA) from PLS-DA projection. Our findings indicate that most sample conditions clustered closely together apart from a slight separation for the knockout cells, indicating that loss of *ERAP1* is associated with larger metabolic changes compared to exposure of high ERAP1 inhibitor levels in this cell line (Fig. 1C and S1 Figure in S1). However, the metabolite features did not map to known metabolites in the database used for annotation.

Using linear models with empirical Bayes moderation and Rubin's rules pooling across three multiple imputation datasets, we compared the control cells to KO and the *ERAP1*-component cells treated with different inhibitor concentrations. In positive ionization mode, we found a total of 25 significantly different metabolite features (P_{adj}<0.05) in *ERAP1*-KO cells (Fig. 2A). None of the other inhibitor conditions revealed statistically significant changes in metabolites after correction for multiple testing, with the exception of 1 feature keto-D-fructose 1,6-bisphosphate [M-H]- that exceeded the threshold for significance (Padj < 0.05, log2-fold change > 2) in the highest inhibitor concentration (50µM) in negative ionization mode (Fig. 2B). This was supported by no differences in the levels of other key metabolite features in positive ionization mode (exploratory analysis), such as carnitine $[M + H]^+$, citrulline $[M + H]^+$, glutamine $[M + H]^+$, histidine $[M + H]^+$, lysine $[M + H]^+$ and some other important metabolites highlighted in (Fig. 3). In addition, inhibitor exposure did not change glutathione $[M + H]^+$ (redox factor) levels, thereby maintaining cellular redox environment that reduces harmful free radicals (Fig. 3)[29], and Sphingosine 1-phosphate $[M + H]^+$ (Sphingolipids) (Fig. 3), a bioactive lipid essential for cell survival (Fig. 3), a bioactive lipid essential for cell survival[30], remained unaffected. We have also tested some key metabolite features in negative ionisation mode such as (R)-lactic acid $[M-H]^-$, aconitic acid $[M-H]^-$, citric acid $[M-H]^-$, Glucose/Fructose-P $[M-H]^-$ and succinic acid $[M-H]^-$ and found no significant differences between the conditions under study (Fig. 4). These results support that ERAP1 inhibition did not significantly alter metabolic homeostasis.

Because we only detected small changes in the ERAP1-KO cells, pathway analysis didn't produce any significant results. Among the significantly different metabolites in the KO condition was choline $[M]^+$, a

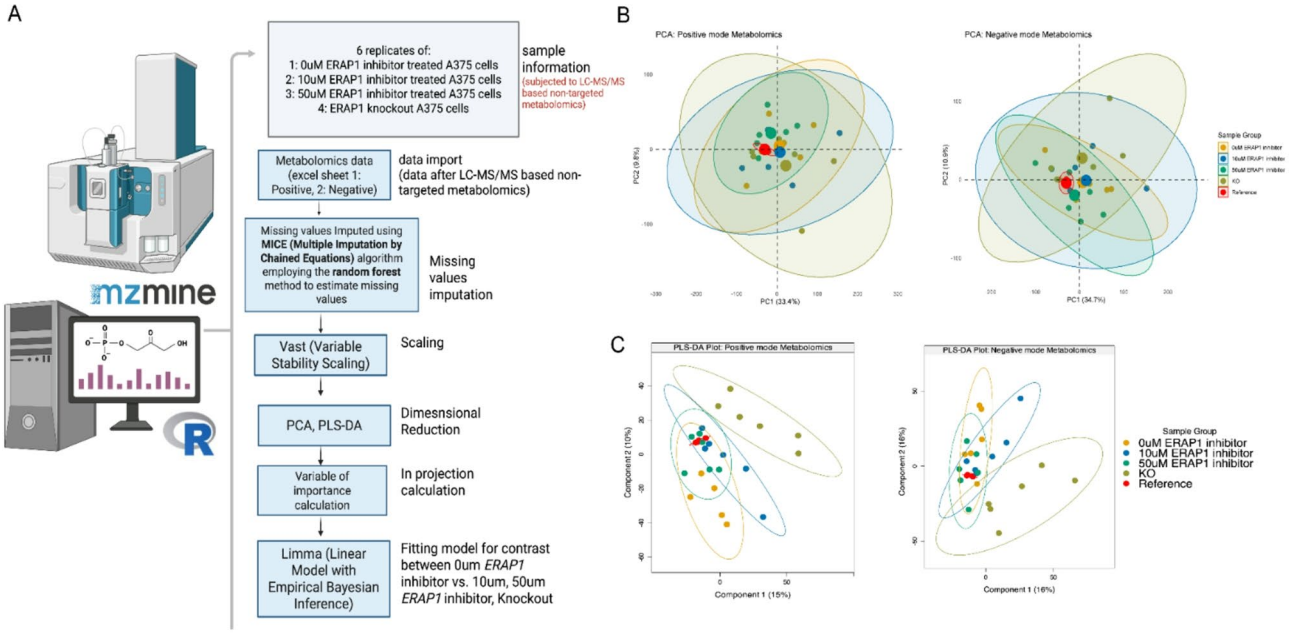

Fig. 1. **A** Overall pipeline used for analysis of metabolomics data, **B** PCA (left for positive, right for negative ionisation mode) (1 C) PLS-DA for positive (left) and negative (right) ionisation mode respectively.

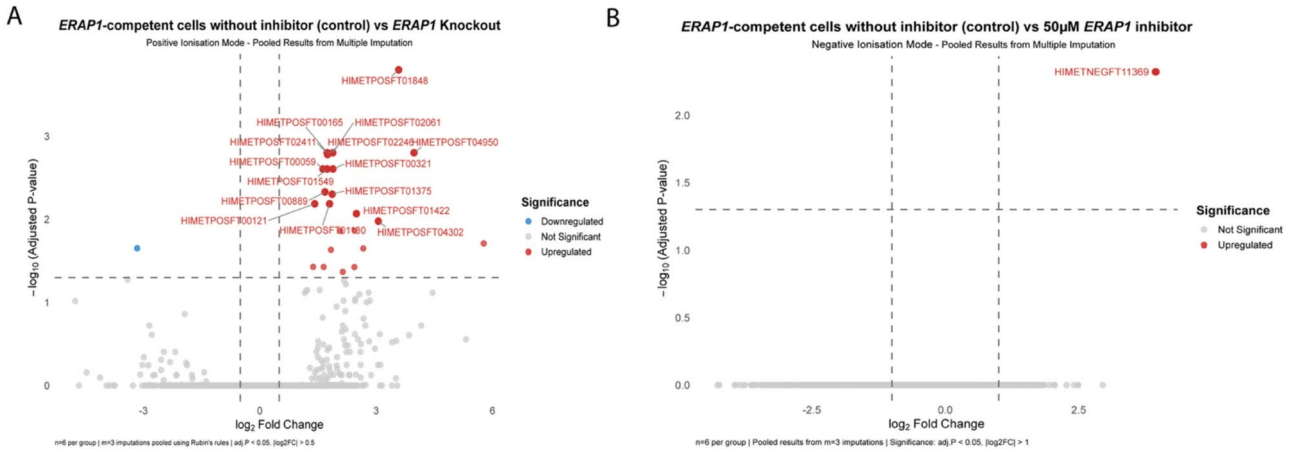

Fig. 2. **A** Volcano plot for comparison of *ERAP1*-component cells without inhibitor (control) with *ERAP1* knockout treated cells in positive ionisation mode. **B** Volcano plot for comparison of *ERAP1*-component cells without inhibitor (control) with 50μM *ERAP1* inhibitor treated cells in negative ionisation mode. ($n = 6$ per group, results pooled across m = 3 imputations and p-values corrected for multiple testing)

vitamin-like amino acid showing higher levels (Fig. 3). Choline is an important metabolite that is involved in shaping antigen presenting cells and regulates inflammatory responses[31]. The increase of choline levels in case of *ERAP1* KO cells may reflect a compensatory metabolic shift triggered by the complete loss of ERAP1 protein.

Overall, even at close to saturating amounts of the allosteric inhibitor, we observe no significant changes in metabolite homeostasis and only limited metabolic perturbations in the absence of the enzyme. ERAP1 has been reported to interact with other proteins in the ER such as ERp44 and ERAP2 and thus any changes unique to the KO cells may be reporting cellular adaptations to lack of the ERAP1 protein and not just its aminopeptidase activity[32,33]. In addition, our results suggest that metabolic effects observed in our previous study[13] are not large enough to be reflected onto metabolite homeostasis. Interestingly, in both studies, ERAP1 deletion resulted in stronger effects compared to pharmacological inhibition, suggesting that the activity of the enzyme is more dispensable than the presence of the intact protein. The differences observed between inhibitor-treated and knockout cells may also stem from the allosteric nature of the inhibitor used, as targeting distinct allosteric sites has previously been shown to produce immunopeptidome patterns that differ from those seen in knockout cells[19].

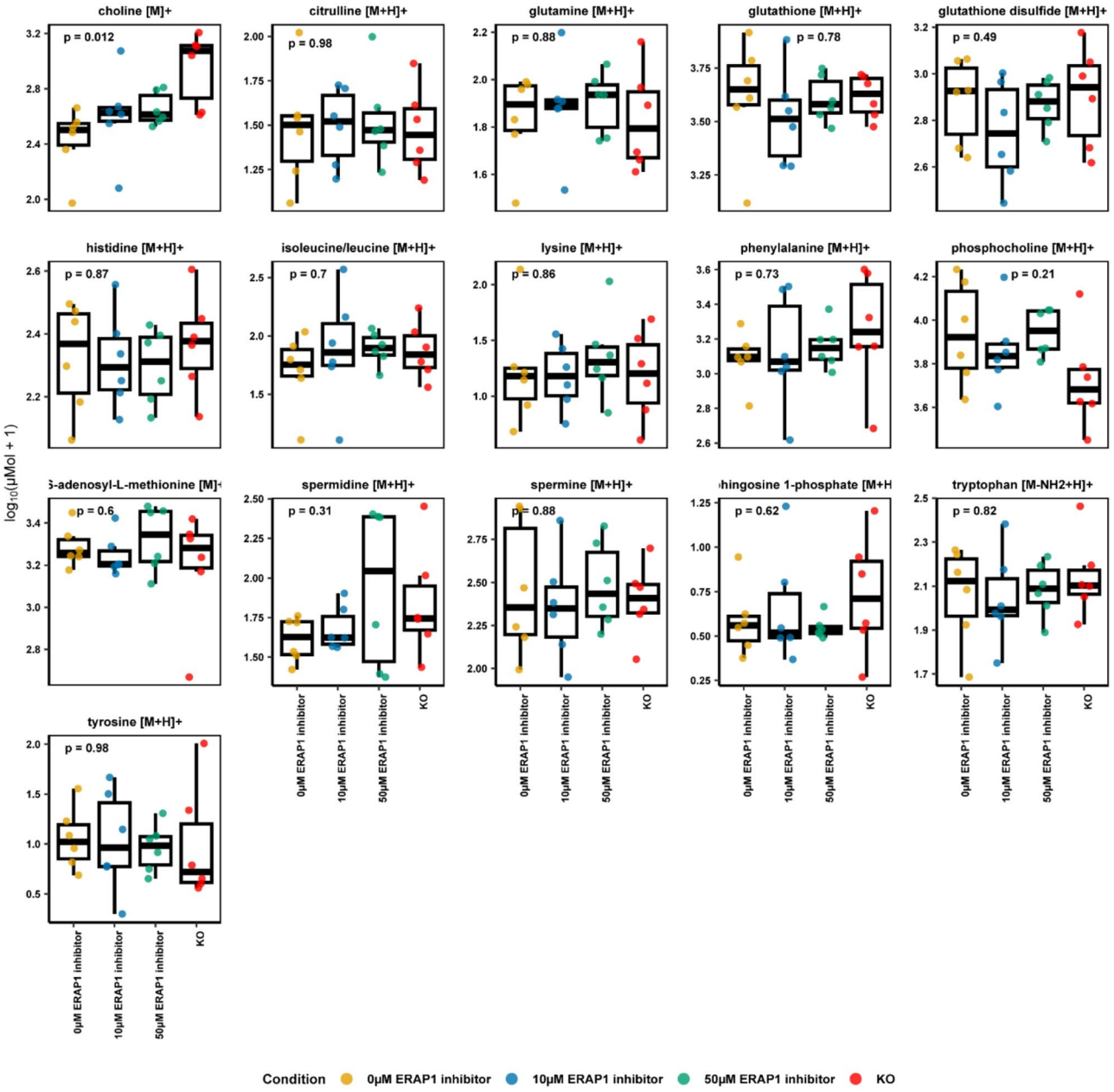

Fig. 3. Boxplots for key annotated metabolite features in positive ionisation mode ($n = 6$ per experimental condition). *P value significance is calculated using ANOVA test (P values from ANOVA are exploratory given limited sample size ($n = 6$ per group provides ~ 28.9% power for medium effects, ~ 13.3% for small effects).

Our study was limited to a single cell line (A375 melanoma cells) since it was inspired from metabolic changes observed in that cell line after ERAP1 inhibition[13]. Although we did not test the metabolic changes upon ERAP1 inhibition or KO in other cell lines, previous analysis of proteomic shifts in THP-1 leukaemia cells upon ERAP1 inhibition has shown similar patterns to A375 cells[13]. Regardless, although our results are reassuring towards lack of significant effects of ERAP1 on metabolite homeostasis, they need to be reproduced in other therapeutically relevant cellular or in vivo systems to establish the safety and efficacy of the approach.

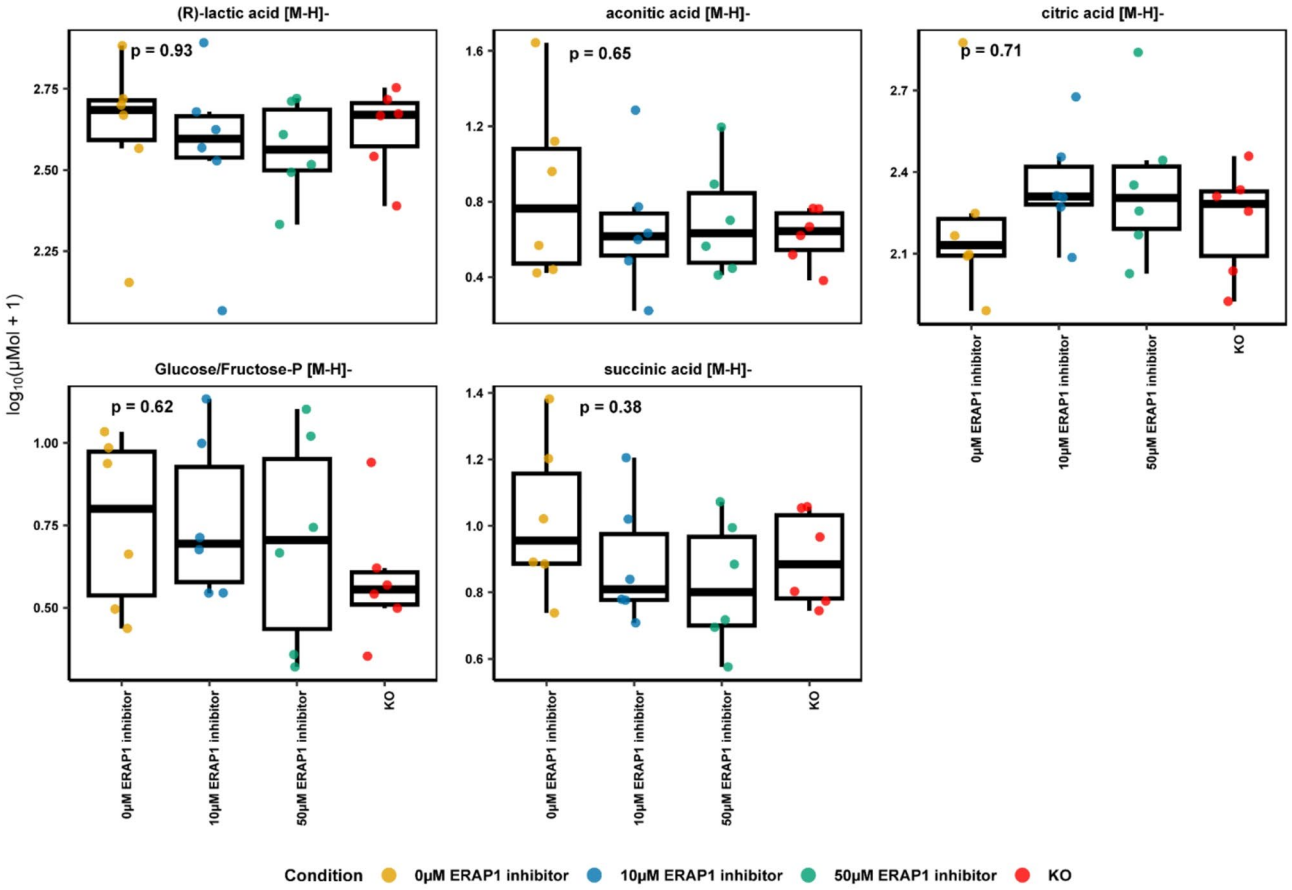

Fig. 4. Boxplots for key annotated metabolite features in negative ionisation mode ($n = 6$ per experimental condition). *p value significance is calculated using ANOVA test (p-values from ANOVA are exploratory given limited sample size ($n = 6$ per group provides ~ 28.9% power for medium effects, ~ 13.3% for small effects).

Conclusion

In conclusion, we show that treatment with an allosteric ERAP1 inhibitor at near saturating concentrations does not significantly alter metabolic homeostasis or induce metabolic toxicity in A375 cells, despite previously reported mitochondrial metabolic effects. While this result is promising for further development of this or similar compounds targeting allosteric sites of this enzyme, additional work will be necessary to establish the general safety of ERAP1 inhibition for therapeutic applications.

Data availability

All data used in this research and scripts used to analyse the data are available in the github repository https://github.com/Araja1234/ERAP1Metabolomics.

Received: 29 October 2025; Accepted: 28 February 2026
Published online: 07 March 2026

References

1. Kuiper, J. J. et al. EULAR study group on MHC-I-opathy: identifying disease-overarching mechanisms across disciplines and borders. *Ann. Rheum. Dis.* **82** (7), 887–896. https://doi.org/10.1136/ard-2022-222852 (2023).
2. James, E., Bailey, I., Sugiyarto, G. & Elliott, T. Induction of protective antitumor immunity through attenuation of ERAAP function. *J. Immunol.* **190** (11), 5839–5846. https://doi.org/10.4049/jimmunol.1300220 (2013).
3. Cifaldi, L. et al. ERAP1 regulates natural killer cell function by controlling the engagement of inhibitory receptors. *Cancer Res.* **75** (5), 824–834. https://doi.org/10.1158/0008-5472.CAN-14-1643 (2015).
4. Tsao, H. W. et al. Targeting the aminopeptidase ERAP enhances antitumor immunity by disrupting the NKG2A-HLA-E inhibitory checkpoint. *Immunity* **57** (12), 2863–2878e12. https://doi.org/10.1016/j.immuni.2024.10.013 (2024).
5. Reeves, E., Islam, Y. & James, E. ERAP1: a potential therapeutic target for a myriad of diseases. *Expert Opin. Ther. Targets.* **24** (6), 535–544. https://doi.org/10.1080/14728222.2020.1751821 (2020).
6. Stratikos, E. Regulating adaptive immune responses using small molecule modulators of aminopeptidases that process antigenic peptides. *Curr. Opin. Chem. Biol.* **23**, 1–7. https://doi.org/10.1016/j.cbpa.2014.08.007 (2014).

7. D'Amico, S. et al. Targeting the antigen processing and presentation pathway to overcome resistance to immune checkpoint therapy. *Front. Immunol.* **13**, 948297. https://doi.org/10.3389/fimmu.2022.948297 (2022).
8. Zervoudi, E. et al. Rationally designed inhibitor targeting antigen-trimming aminopeptidases enhances antigen presentation and cytotoxic T-cell responses. *Proc. Natl. Acad. Sci. USA* **110** (49), 19890–19895. https://doi.org/10.1073/pnas.1309781110 (2013).
9. Kokkala, P. et al. Optimization and structure-activity relationships of phosphinic pseudotripeptide inhibitors of aminopeptidases that generate antigenic peptides. *J. Med. Chem.* **59** (19), 9107–9123. https://doi.org/10.1021/acs.jmedchem.6b01031 (2016).
10. Vourloumis, D. et al. Discovery of selective nanomolar inhibitors for insulin-regulated aminopeptidase based on α-hydroxy-β-amino acid derivatives of bestatin. *J. Med. Chem.* **65** (14), 10098–10117. https://doi.org/10.1021/acs.jmedchem.2c00904 (2022).
11. Giastas, P., Neu, M., Rowland, P. & Stratikos, E. High-resolution crystal structure of endoplasmic reticulum aminopeptidase 1 with bound phosphinic transition-state analogue inhibitor. *ACS Med. Chem. Lett.* **10** (5), 708–713. https://doi.org/10.1021/acsmedchemlett.9b00002 (2019).
12. Maben, Z. et al. Discovery of selective inhibitors of endoplasmic reticulum aminopeptidase 1. *J. Med. Chem.* **63** (1), 103–121. https://doi.org/10.1021/acs.jmedchem.9b00293 (2020).
13. Nikopaschou, M. et al. ERAP1 activity modulates the immunopeptidome but also affects the proteome, metabolism, and stress responses in cancer cells. *Mol. Cell. Proteom.* **24** (5), 100964. https://doi.org/10.1016/j.mcpro.2025.100964 (2025).
14. Schott, B. H. et al. Single-cell genome-wide association reveals that a nonsynonymous variant in ERAP1 confers increased susceptibility to influenza virus. *Cell. Genom.* **2** (11), 100207. https://doi.org/10.1016/j.xgen.2022.100207 (2022).
15. Liu, H. et al. Endoplasmic reticulum aminopeptidase 1 is involved in anti-viral immune response of hepatitis B virus by trimming hepatitis B core antigen to generate 9-mers peptides. *Front. Microbiol.* **13**, 829241. https://doi.org/10.3389/fmicb.2022.829241 (2022).
16. Wang, X. et al. STING agonist-based ER-targeting molecules boost antigen cross-presentation. *Nature* **641** (8061), 202–210. https://doi.org/10.1038/s41586-025-08758-w (2025).
17. Zong, L., Xing, J., Liu, S., Liu, Z. & Song, F. Cell metabolomics reveals the neurotoxicity mechanism of cadmium in PC12 cells. *Ecotoxicol. Environ. Saf.* **147**, 26–33. https://doi.org/10.1016/j.ecoenv.2017.08.028 (2018).
18. Halama, A. Metabolomics in cell culture—a strategy to study crucial metabolic pathways in cancer development and the response to treatment. *Arch. Biochem. Biophys.* **564**, 100–109. https://doi.org/10.1016/j.abb.2014.09.002 (2014).
19. Temponeras, I. et al. Distinct modulation of cellular immunopeptidome by the allosteric regulatory site of ER aminopeptidase 1. *Eur. J. Immunol.* **53** (8), e2350449. https://doi.org/10.1002/eji.202350449 (2023).
20. Artati, A., Couacault, P. & Witting, M. Nontargeted metabolomics using the sciex zenoTOF 7600. *Methods Mol. Biol.* **2925**, 1–23. https://doi.org/10.1007/978-1-0716-4534-5_1 (2025).
21. Buuren, S. V. & Groothuis-Oudshoorn, K. mice: multivariate imputation by chained equations in *R. J. Stat. Soft.* **45** (3). https://doi.org/10.18637/jss.v045.i03 (2011).
22. Keun, H. C. et al. Improved analysis of multivariate data by variable stability scaling: application to NMR-based metabolic profiling. *Anal. Chim. Acta.* **490** (1), 265–276. https://doi.org/10.1016/S0003-2670(03)00094-1 (2003).
23. Lê, S., Josse, J. & Husson, F. FactoMineR: an R package for multivariate analysis. *J. Stat. Softw.* **25**, 1–18. https://doi.org/10.18637/jss.v025.i01 (2008).
24. Rohart, F., Gautier, B., Singh, A. & Cao, K. A. L. mixOmics: an R package for 'omics feature selection and multiple data integration. *PLoS Comput. Biol.* **13** (11), e1005752. https://doi.org/10.1371/journal.pcbi.1005752 (2017).
25. Ritchie, M. E. et al. limma powers differential expression analyses for RNA-sequencing and microarray studies. *Nucleic Acids Res.* **43** (7), e47. https://doi.org/10.1093/nar/gkv007 (2015).
26. Benjamini, Y. & Hochberg, Y. Controlling the false discovery rate: a practical and powerful approach to multiple testing. *J. R. Stat. Soc. Ser. B (Methodological)* **57** (1), 289–300 (1995).
27. Fahy, E. & Subramaniam, S. RefMet: a reference nomenclature for metabolomics. *Nat. Methods.* **17** (12), 1173–1174. https://doi.org/10.1038/s41592-020-01009-y (2020).
28. Wishart, D. S. et al. HMDB: the human metabolome database. *Nucleic Acids Res.* **35** (Database issue), D521–526. https://doi.org/10.1093/nar/gkl923 (2007).
29. Wu, G., Lupton, J. R., Turner, N. D., Fang, Y. Z. & Yang, S. Glutathione metabolism and its implications for health. *J. Nutr.* **134** (3), 489–492. https://doi.org/10.1093/jn/134.3.489 (2004).
30. Oh, J. et al. Deep sphingolipidomic and metabolomic analyses of ceramide synthase 2 null mice reveal complex pathway-specific effects. *J. Lipid Res.* **66** (7), 100832. https://doi.org/10.1016/j.jlr.2025.100832 (2025).
31. Maia, C., Fung, C. W. & Sanchez-Lopez, E. Choline in immunity: a key regulator of immune cell activation and function. *Front. Immunol.* **16** https://doi.org/10.3389/fimmu.2025.1617077 (2025).
32. Hisatsune, C. et al. ERp44 exerts redox-dependent control of blood pressure at the ER. *Mol. Cell.* **58** (6), 1015–1027. https://doi.org/10.1016/j.molcel.2015.04.008 (2015).
33. Evnouchidou, I., Weimershaus, M., Saveanu, L. & van Endert, P. ERAP1-ERAP2 dimerization increases peptide-trimming efficiency. *J. Immunol.* **193** (2), 901–908. https://doi.org/10.4049/jimmunol.1302855 (2014).

Acknowledgements

This project has received funding from the European Union's Horizon 2020 research and innovation programme under the Marie Skłodowska-Curie grant agreement No 954992.

Author contributions

A.R. analysed the data and wrote the manuscriptM.N. performed experiments and reviewed the manuscript-J.H.B. reviewed the manuscriptJ.O.N . reviewed the manuscriptA.A. performed experimentsM.W. Performed experiments, reviewed and supervised the projectE.S. wrote, reviewed and supervised the projectJ.J.W.K. wrote, reviewed and supervised the project.

Funding

This project has received funding from the European Union's Horizon 2020 research and innovation programme under the Marie Skłodowska-Curie grant agreement No 954992.

Declarations

Competing interests

The authors declare no competing interests.

Additional information

Supplementary Information The online version contains supplementary material available at https://doi.org/10.1038/s41598-026-42975-1.

Correspondence and requests for materials should be addressed to E.S. or J.J.W.K.

Reprints and permissions information is available at www.nature.com/reprints.

Publisher's note Springer Nature remains neutral with regard to jurisdictional claims in published maps and institutional affiliations.